The Precession Index, A Nonlinear Energy Balance Model, And Seversmith Psychroterms

by

David Parry Rubincam

POPULAR SUMMARY

An important component of Milankovitch's astronomical theory of climate change is the precession index. The precession index, along with the Earth's tilt and orbital eccentricity, are believed to be the major controlling factors of climate change in the last few million years. The precession index is $e \sin \omega_S$ where e is the Earth's orbital eccentricity and ω_S measures how close the Sun is to the Earth at midsummer. When $\omega_S = 90°$ the Sun is close to the Earth during northern summer, and at 270° it is far from the Earth during northern summer. The precession index varies with time, because both the eccentricity e and the parameter ω_S are constantly changing due to disturbances in the Earth's orbit by other planets, and due to the precession of the Earth. The change is largely periodic, with a period of about 23,000 years.

This 23,000 year period is in fact observed in the paleoclimate record; deep-sea cores of the ooze at the bottom of the ocean clearly show that ice volume during the ice ages fluctuates with a 23,000 year period. (Ice volume also fluctuates with other astronomical periods: at 100,000 years, possibly due to changes in e alone, and at 41,000 years due to changes in the Earth's tilt.)

The standard explanation for the importance of the precession index is that cool northern summers are required for the growth of ice. The idea is that snow lingers through

the summer when the Sun is far from the Earth during northern summer, and ultimately builds up into ice sheets in northern Canada and Siberia. In this sense the northern hemisphere would be said to "control" the ice ages.

In this paper I challenge the standard point of view. The examination of the simplest nonlinear energy balance climate model indicates that it is a seemingly paradoxical cooling of the southern oceans when the Sun's perihelion is over the southern hemisphere (and therefore far from the northern hemisphere during northern summer) that causes ice to accumulate. This "paradoxical" cooling is an inevitable consequence of the simplest climate models. The cold water eventually flows north, cooling the northern hemisphere to the point where ice can form. In arguing for this point of view I cite evidence that the southern oceans cool before the northern oceans. In this sense the southern hemisphere can be said to "control" the precession index ice sheets. I find for the simple climate model considered here that the change in temperature between ice ages and temperate times can reach as much as 0.6° C. Presumably better climate models can increase the temperature difference even more. For comparison, the global average difference in temperature between now and the last glacial maximum was about 4° C.

The Precession Index, A Nonlinear Energy Balance Model, And Seversmith Psychroterms

by

David Parry Rubincam

Geodynamics Branch, Code 921
Laboratory for Terrestrial Physics
NASA Goddard Space Flight Center
Building 33, Room G308
Greenbelt, MD 20771

voice: 301-614-6464
fax: 301-614-6522
email: David.P.Rubincam@nasa.gov

12 February 2004

Abstract

A simple nonlinear energy balance climate model yields a precession index-like term in the temperature. Despite its importance in the geologic record, the precession index e sin ω_S, where e is the Earth's orbital eccentricity and ω_S is the Sun's perigee in the geocentric frame, is not present in the insolation at the top of the atmosphere. Hence there is no one-for-one mapping of 23,000 and 19,000 year periodicities from the insolation to the paleoclimate record; a nonlinear climate model is needed to produce these long periods. A nonlinear energy balance climate model with radiative terms of form T^n, where T is surface temperature and $n > 1$, does produce e sin ω_S terms in temperature; the e sin ω_S terms are called Seversmith psychroterms. Without feedback mechanisms, the model achieves extreme values of ±0.64 K at the maximum orbital eccentricity of 0.06, cooling one hemisphere while simultaneously warming the other; the hemisphere over which perihelion occurs is the cooler. In other words, the nonlinear energy balance model produces long-term cooling in the northern hemisphere when the Sun's perihelion is near northern summer solstice and long-term warming in the northern hemisphere when the aphelion is near northern summer solstice. (This behavior is similar to the inertialess gray body which radiates like T^4, but the amplitude is much lower for the energy balance model because of its thermal inertia.) This seemingly paradoxical behavior works against the standard Milankovitch model, which requires cool northern summers (Sun far from Earth in northern summer) to build up northern ice sheets, so that if the standard model is correct it must be more efficient than previously thought. Alternatively, the new mechanism could possibly be dominant and indicate southern hemisphere control of the northern ice sheets, wherein the southern oceans undergo a long-term cooling when the Sun is far from the Earth during northern summer. The cold water eventually flows north, cooling the northern hemisphere. This might explain why the northern oceans lag the southern ones when it comes to orbital forcing.

1. Introduction

A previous paper [*Rubincam*, 2004] examined the simplest possible climate model: that of a gray body with a uniform surface albedo and infrared emissivity, but without thermal inertia. The gray body emits infrared radiation like T^4, where T is surface temperature. It was found that the nonlinearity in T produced surface temperature terms, called Seversmith psychroterms, which have the form $e \sin \omega_S$, the same as Milankovitch's precession index; here e is the Earth's orbital eccentricity and ω_S is the argument of perigee of the Sun's orbit about the Earth (see Figure 1). It was suggested that the psychroterms were the cause of the ices ages which come and go with $e \sin \omega_S$, rather than *Milankovitch's* [1941] traditional mechanism. The results of *Rubincam* [2004] also suggested a program of examining more and more complicated climate models to see how the psychroterms fare in them.

Accordingly, the present paper examines the next simplest climate model up from the gray body: the nonlinear energy balance model (NEBM). The NEBM also radiates nonlinearly with T, but does have a thermal inertia-type term, which the gray body lacked. It is found here that the $e \sin \omega_S$ psychroterms are still present, but reduced by an order-of-magnitude due to the presence of thermal inertia, to about ± 0.64 K when $e = 0.06$. No ice-albedo feedback is assumed. Ice-albedo feedback might magnify the effect by a factor of several up to perhaps one or a few K, which would seem to be enough to produce an ice age. Paleoclimate data in support of the Seversmith psychroterms as the cause of the precession index ice ages is discussed blow.

The precession index is an important component of *Milankovitch's* [1941] astronomical theory of climate change [e.g., *Hays et al.* 1976; *Berger et al.* 1984; *Hinnov* 2000]. Once again, the precession index is $e \sin \omega_S$, where e is the Earth's orbital eccentricity and ω_S is the argument of perigee of the Sun's orbit about the Earth. The orbital geometry is given in Figure 1; note that a geocentric reference frame is assumed, so

that the Sun is treated as a satellite of the Earth, just as it was in two previous papers [*Rubincam* 1994, 2004]. In this frame the Sun is close to the northern hemisphere when $\omega_S = 90°$ and the Sun is at northern summer solstice. Likewise, the Sun is far from the northern hemisphere when $\omega_S = 270°$ and the Sun is at northern summer solstice. The precession index spectrum has a major peak at 23 kyr and a smaller one at 19 kyr (1 kyr = 1000 years).

It is an interesting fact that the equation for the insolation at the top of the atmosphere contains no terms which look like the precession index $e \sin \omega_S$, a result demonstrated by *Humphreys* [1964, pp. 85-87], and rediscovered by *Rubincam* [1994; 1996] and Bruce G. Bills (private communication, 1994); see also *Hinnov* [2000] and *Rubincam* [2004]. Terms which have the form $e \sin \omega_S$ have been christened psychroterms [*Rubincam*, 2004], from the Greek word "psychro," meaning "cold." Thus the $e \sin \omega_S$ term in the insolation, called the Humphreys psychroterm [*Rubincam*, 2004], was demonstrated by W. J. Humphreys to be zero. Therefore the insolation equation does not contain the 23 kyr and 19 kyr periods associated with $e \sin \omega_S$. Because of its undoubted importance in the paleoclimate record, the existence of the precession index must be due to the Earth's nonlinear response to the insolation.

The standard explanation for the importance of the precession index $e \sin \omega_S$ is that cool northern summers ($\omega_S \approx 270°$, $M_S \approx 180°$) allow snow to linger into the summer. Positive ice-albedo feedback feeds the growth of ice, ultimately building up into the major ice sheets [e.g., *Milankovitch*, 1941, pp. 435-436; *Pisias and Imbrie*, 1986]. This mechanism thus invokes a nonlinear response to obtain the 23 kyr and 19 kyr frequencies in ice volume [*Rubincam*, 1996; 2004]. Moreover, the standard "model" given by *Milankovitch* [1941] is questionable: he uses the dubious notion of caloric half-years (p. 414), and then correlates the snow line with summer insolation and calls the correlation "proof" (p. 436).

A previous paper [*Rubincam*, 2004] examined the simplest of all possible climate models: the gray body without thermal inertia, and where albedo A and infrared emissivity ε_{IR} are constants across its surface. The equation of the inertialess gray body is

$$\varepsilon_{IR}\sigma T^4 = (1 - A)F_S \tag{1}$$

where T is absolute temperature, F_S is the insolation and $\sigma = 5.67 \times 10^{-8}$ $Wm^{-2}K^{-4}$ is the Stefan-Boltzmann constant. Because the gray body radiates like T^4, it is a nonlinear climate model and does produce e sin ω_S terms in temperature T from the e sin ω_S-free insolation. Any e sin ω_S terms in temperature are called Seversmith psychroterms [*Rubincam*, 2004] to distinguish them from the Humphreys psychroterm in the insolation, which, as stated before, is zero.

The present paper examines a slightly more complicated model: a nonlinear energy balance model, which radiates according to T, T^2, T^3, and T^4 terms. Unlike the inertialess gray body examined in *Rubincam* [2004], the nonlinear energy balance model does have thermal inertia.

In order to solve the NEBM equation (NEBM = nonlinear energy balance model), temperature is written as $T = T_0 + \Delta T$ and T^n is expanded to order $(\Delta T)^2$. Like the gray body given by (1), the NEBM has a major Seversmith psychroterm term of the form $\Delta T_{SP} \propto$ $-e$ sin ω_S $P_1(\sin \phi)$ in the surface temperature, with a small contribution from a similar $P_3(\sin \phi)$ term. Here $P_\ell(\sin \phi)$ is the Legendre polynomial of degree ℓ, ϕ is latitude, and the subscript "SP" on ΔT stands for "Seversmith psychroterm." The magnitude of the temperature change can reach extremes about ±0.64 K at latitudes ±48.5° for the NEBM for the sum of the first two Seversmith psychroterms when the eccentricity e reaches its maximum value of 0.06 and $\omega_S = 90°$ or 270°. No ice-albedo feedback is assumed.

Because $P_1(\sin\phi) = \sin\phi$ and $P_3(\sin\phi) = (5\sin^3\phi - 3\sin\phi)/2$, both of which change sign when the equator is crossed, the NEBM indicates simultaneous warming in one hemisphere and cooling in the other; the hemisphere over which perihelion occurs is the cooler. In other words, it yields precession index-type terms in T with a seemingly paradoxical sign: long-term cooling in the northern hemisphere when the Sun is near perihelion during northern summer ($\omega_S \approx 90°$) and a long-term warming in the north when the Sun is near aphelion during northern summer ($\omega_S \approx 270°$). The gray body does the same for the same reason [*Rubincam*, 2004].

The paradox is resolved by noting the following. Suppose perihelion occurs at $\omega_S = 270°$, so that perihelion is achieved over the southern hemisphere. Although the Sun is closer to the southern hemisphere with this geometry, the Sun does not spend much time there, because by Kepler's second law the Sun moves fastest when it is closest to the Earth. On the other hand, the Sun lingers near aphelion, producing a long, cold winter in the south. The net result is that, on the average, the southern hemisphere is cooler.

This effect thus works in opposition to the usual Milankovitch explanation of $e \sin\omega_S$, wherein cool summers (Sun far from Earth during northern summer) are required for the snow linger in order to build up into ice sheets in Canada and Fennoscandia. In this case the psychroterms warm the ground during the cool northern summers, making it harder for the standard model to work.

The results of *Rubincam* [2004] and the present investigation suggest an alternative explanation for the $e \sin\omega_S$, ice ages: the long-term cooling of the southern ocean when $\omega_S \approx 270°$ may be the trigger for the northern ice sheets. Perhaps sea ice around Antarctica causes ice-albedo feedback [*Gildor and Tziperman*, 2000, 2001] which cools the water even more; the cold water makes its way north, cooling the northern hemisphere and causing the ice sheets to grow.

This could possibly explain the phase shift seen in the sea surface temperatures for the precession index, as discussed by *Imbrie et al.* [1988, pp. 144-148]. They note that the

northern oceans significantly lag the southern oceans with respect to the orbital forcing. This is what would be expected from the southern oceans cooling first, and then the northern as the cold waters spread north. Because the turn-over time of the oceans is a few thousand years, the northern hemisphere should lag the southern by this amount. This is what is observed (see the Discussion). There is some support for this point of view in the obliquity forcing as well; here also the northern oceans lag the southern in the obliquity forcing [*Imbrie et al.*,1988, pp. 147-148], again arguing for southern ocean control of the ice ages. Climate models more sophisticated than that examined here would be needed to pursue this idea further.

2. Insolation

The insolation expressed in terms of the orbital parameters is given by

$$F_S = F_S^0\left(\frac{r_0}{a}\right)^2 \sum_{\ell=0}^{\infty} d_\ell \sum_{m=0}^{\ell} (2-\delta_{0m}) \frac{(\ell-m)!}{(\ell+m)!} P_{\ell m}(\sin\phi)$$
$$\bullet \sum_{p=0}^{\ell} \sum_{q=-\infty}^{+\infty} F_{\ell mp}(\varepsilon)\, W_{\ell-2p,q}(e)$$
$$\bullet \begin{bmatrix}\cos\\ \sin\end{bmatrix}_{\ell-m\,odd}^{\ell-m\,even} [(\ell-2p)\omega_S + (\ell-2p+q)M_S + m(\Omega_S-\eta-\lambda)] \qquad (2)$$

[*Rubincam*, 1994, 2004]. Here $F_S^0 = 1371$ W m^{-2} when the reference distance r_0 is $r_0 = a =$ 1 AU [*Hickey et al.*, 1988], where a is the semimajor axis of the Earth's orbit. Also, e is orbital eccentricity, ω_S is the argument of perigee, M_S is the mean anomaly of the Sun's orbit about the Earth (see Figure 1), and Ω_S is the position of the line of nodes of the Sun's orbit measured from the vernal equinox; $\Omega_S = 0$ hereafter. The angle ε is the Earth's obliquity (currently about 23.44°), and ϕ is latitude and λ is east longitude on the Earth,

while η is Greenwich sidereal time. The $P_{\ell m}(\sin \phi)$ are the associated Legendre polynomials of degree ℓ and order m. The d_ℓ are spherical harmonic coefficients given in *Rubincam* [1994, Table 1]. The first few values are $d_0 = 1/4$, $d_1 = 1/2$, $d_2 = 5/16$, and $d_4 = -3/32$. All the d_ℓ with odd subscripts are zero except for d_1. The $F_{\ell mp}(\varepsilon)$ are the inclination functions from celestial mechanics; *Rubincam* [1994, Table 2; 2004, Table 2] gives them for degree 1, while *Kaula* [1966] and *Caputo* [1967] list them for degrees 2 through 4. The $W_{\ell\text{-}2p,q}(e)$ are not the eccentricity functions from celestial mechanics; rather, they are special eccentricity functions associated solely with the insolation and are tabulated in *Rubincam* [1994]. (There is a typographical error in Table 3 of that paper; the entry for $\ell - 2p = \pm 1$, $q = \pm 1$ should read $2e - 3e^3/2$ instead of $2e - 3e^4/2$. Also, the $(2^\ell - 2s)!$ factor in the equation following (7) in the same paper should read $(2\ell - 2s)!$.)

The zonal insolation can be found from (2) by setting $m = 0$. The zonal insolation given by equation (8) in *Rubincam* [1994] contains some errors. The corrected equation for the zonal insolation at the top of the atmosphere is

$$
\begin{aligned}
F_S \;=\; & F_S^0 \left(\frac{r_0}{a}\right)^2 \\
& \bullet \left\{ \frac{1}{4} P_0(\sin\phi) \bullet \left[1 \;+\; \frac{e^2}{2} \;+\; 2e\cos M_S \;+\; \frac{5}{2} e^2 \cos 2M_S \right] \right. \\
& \left. +\; \frac{1}{2} P_1(\sin\phi) \right. \\
& \qquad \bullet \left[\left(1 - \frac{e^2}{2}\right) \sin\varepsilon \sin(\omega_S + M_S) \;+\; 2e \sin\varepsilon \sin(\omega_S + 2M_S) \right. \\
& \qquad \left. \left. +\; \frac{e^2}{8} \sin\varepsilon \sin(\omega_S - M_S) \;+\; \frac{27}{8} e^2 \sin\varepsilon \sin(\omega_S + 3M_S) \right] \right\}
\end{aligned}
$$

$$+ \frac{5}{16} P_2(\sin\phi)$$

$$\bullet\Big[(1+\frac{e^2}{2})(\frac{3}{4}\sin^2\varepsilon - \frac{1}{2}) - \frac{3}{4}(1-\frac{7}{2}e^2)\sin^2\varepsilon\cos(2\omega_S + 2M_S)$$

$$+ 2e(\frac{3}{4}\sin^2\varepsilon - \frac{1}{2})\cos M_S + \frac{3}{4}e\sin^2\varepsilon\cos(2\omega_S + M_S)$$

$$- \frac{9}{4}e\sin^2\varepsilon\cos(2\omega_S + 3M_S) + \frac{5}{2}e^2(\frac{3}{4}\sin^2\varepsilon - \frac{1}{2})\cos 2M_S$$

$$- \frac{39}{8}e^2\sin^2\varepsilon\cos(2\omega_S + 4M_S)\Big] + \ldots\Big\} \qquad (3)$$

to order e^2. The $P_\ell(\sin\phi)$ are the usual Legendre polynomials

$$P_0(\sin\phi) = 1 ,$$

$$P_1(\sin\phi) = \sin\phi ,$$

$$P_2(\sin\phi) = \frac{3}{2}\sin^2\phi - \frac{1}{2} ,$$

$$P_3(\sin\phi) = \frac{5}{2}\sin^3\phi - \frac{3}{2}\sin\phi ,$$

etc. Being just the zonal (longitude-independent) insolation, the diurnal, semidiurnal, etc. terms are not given in (3); but they are contained in (2) in the $m \neq 0$ terms.

The important thing to notice about (3) is that it does *not* contain a term of the form

$$F_S = \ldots + \textit{coefficient} \times e\sin\omega_S + \ldots .$$

In other words, there is no term in the insolation which looks like the precession index. Hence there is no term in the insolation at the top of the atmosphere which has periods of 23 kyr and 19 kyr. Bruce G. Bills, in an independent analysis (unpublished, 1994), arrived at the same conclusion. This lack of a precession index in the insolation was in fact demonstrated early on by *Humphreys* [1964, pp. 85-87] in his classic book on meteorology; Rubincam and Bills rediscovered his result via more sophisticated mathematics.

The only thing in (3) which even remotely looks like the precession index is the $2e$ sin ε sin $(\omega_S + 2M_S)$ term which multiplies $P_1(\sin \phi)$. However, this term has a high frequency due to the presence of the $2M_S$. Its period is about half a year, not 19 kyr or 23 kyr.

This result has caused some confusion [*Berger*, 1996; *Rubincam*, 1996; *Hinnov*, 2000] because 23 kyr and 19 kyr periods are strongly indicated in the paleoclimate records [e.g., *Hays et al.*, 1976; *Berger et al.*, 1984]. If the Milankovitch theory of climate is correct, how can there be an e sin ω_S signal in the paleoclimate records when it does not exist in the insolation?

The answer is that if e sin ω_S is important for climate, it must be due to the way the Earth responds to the insolation [*Rubincam*, 1994, 1996, 2004]. In other words, the Earth's climate system does something nonlinear to the astronomical signal, thereby manufacturing the 23 kyr and 19 kyr periods. *Rubincam* [1994, p. 201] produced a model which in fact gave a precession index-like term in the radiation reaching the ground. That radiation is the insolation at the top of the atmosphere multiplied by the Earth's coalbedo (coalbedo = $1 - A$, where A is the albedo). Short-period terms in the albedo can multiply short-period terms in the insolation, eliciting e sin ω_S. But this "precession index" was extremely weak. On the other hand, the gray body elicits huge Seversmith psychroterms,

due the strong T^4 dependence of emitted radiation on temperature, and the tremendous temperature extremes caused by a lack of thermal inertia [*Rubincam*, 2004].

A simple nonlinear energy balance model (NEBM) is examined below; it produces e sin ω_S in the Earth's temperature and has extreme values of about ± 0.64 K at latitudes ±48.5° when the Earth's orbital eccentricity is at its maximum value of $e = 0.06$ and $\omega_S =$ 90° or 270°. These values are comparable to those induced by obliquity variations. No ice-albedo feedback is assumed.

3. Nonlinear energy balance climate model

The zonal nonlinear energy balance climate model (NEBM) is [e.g., *North et al.*, 1981, 1983]:

$$C\frac{\partial T}{\partial t} - \frac{\partial\left[D(1-\mu^2)\frac{\partial T}{\partial \mu}\right]}{\partial \mu} + B_0 + \sum_{i=1}^{4} B_i T^i = (1-A)F_S \qquad (4)$$

where $\mu = \sin \phi$ and the $B_i T^i$ terms for $i \geq 2$ are added nonlinear terms not given by North *et al.*, and where now T is surface temperature in degrees Centigrade instead of the absolute temperature. Only the zonal terms will be needed, since the short-period diurnal terms will be largely damped out by the heat storage term which was not present in the inertia-free gray body [*Rubincam*, 2004] . The time t is measured in tropical years, so that $\omega_S + M_S$ has a frequency of 2π.

The first term $C\partial T/\partial t$ in the equation above represents heat storage where C is a kind of heat capacity; thus this terms produces the thermal inertia. The second term represents zonal diffusion as produced by winds and ocean currents and has a diffusion constant D. The infrared radiation leaving the Earth in the above equation is given by

$$I = B_0 + B_1 T + B_2 T^2 + B_3 T^3 + B_4 T^4 \tag{5}$$

The values for the B_i can be estimated from the data of *Graves et al.* [1993] (see Figure 2); these values are $B_0 = 195.0$, $B_1 = 1.4158$, $B_2 = 0.02289$, $B_3 = 0.001148$, and $B_4 = 0.00002089$. These numbers do not come from a least-squares fit; rather, they were chosen to bisect the envelope of the data.

The linearized version of (4) will be solved for first. Writing

$$T = T_0 + \Delta T \tag{6}$$

gives by (5)

$$I = H_0 + \sum_{i=1}^{4} H_i (\Delta T)^i \tag{7}$$

where

$$H_0 = B_0 + B_1 T_0 + B_2 T_0^{\,2} + B_3 T_0^{\,3} + B_4 T_0^{\,4}$$

$$H_1 = B_1 + 2B_2 T_0 + 3B_3 T_0^{\,2} + 4B_4 T_0^{\,3}$$

$$H_2 = B_2 + 3B_3 T_0 + 6B_4 T_0^{\,2}$$

$$H_3 = B_3 + 4B_4 T_0$$

$$H_4 = B_4$$

and now $T_0 = 14.9$ °C. [*North et al.*, 1981, Table 1], with $H_0 = 226.005$, $H_1 = 3.1389$, $H_2 = 0.1020$, $H_3 = 0.00235$, and $H_4 = 0.00002089$. The linearized, first-order equation is then

$$C\frac{\partial(T_0+\Delta T)}{\partial t} - \frac{\partial\left[D(1-\mu^2)\dfrac{\partial(T_0+\Delta T)}{\partial\mu}\right]}{\partial\mu} + H_0 + H_1\Delta T \cong (1-A)\left[\frac{F_S^0}{4}\left(\frac{r_0}{a}\right)^2 + \Delta F_S\right] \tag{8}$$

where by (3)

$$\begin{aligned}\Delta F_S &= F_S^0\left(\frac{r_0}{a}\right)^2\left\{\frac{1}{4}P_0(\sin\phi)\bullet\left[2e\cos M_S\right]\right.\\ &+ \frac{1}{2}P_1(\sin\phi)\bullet\left[\sin\varepsilon\sin(\omega_S+M_S) + 2e\sin\varepsilon\sin(\omega_S+2M_S)\right]\\ &+ \frac{5}{16}P_2(\sin\phi)\bullet\left[\left(\frac{3}{4}\sin^2\varepsilon-\frac{1}{2}\right)\left(1+2e\cos M_S\right)\right.\\ &+ \left.\left.\frac{3}{4}e\sin^2\varepsilon\left(\cos(2\omega_S+M_S)-3\cos(2\omega_S+3M_S)\right)\right]\right\}. \end{aligned}\tag{9}$$

This equation is truncated at the first power in e and at $\ell = 2$. This is the usual form of the energy balance model and can be solved in the usual manner [*North et al.*, 1981]. Setting

$$H_0 = (1-A)Q$$

where

$$Q = \frac{F_S^0}{4}\left(\frac{r_0}{a}\right)^2$$

allows the albedo A to be solved for, giving $A = 0.344$, in reasonable agreement with the observed value of 0.30 [*Stephens et al.*, 1981], and leaving the linear equation

$$C\frac{\partial(\Delta T)}{\partial t} - \frac{\partial\left[D(1-\mu^2)\frac{\partial(\Delta T)}{\partial \mu}\right]}{\partial \mu} + H_1 \Delta T \cong (1-A)\Delta F_S \ . \qquad (10)$$

In this equation ΔT will be assumed to have the same form as the zonal ΔF_S as given by (9), except that the parts which have a period of about a year are lagged by an angle ψ:

$$\begin{aligned}\Delta T = {} & \frac{\tau_1}{2} e \cos(M_S - \psi) \\ & + \frac{\tau_1}{2} P_1(\sin\phi) \sin\varepsilon \sin(\omega_S + M_S - \psi) \\ & + \frac{5}{16}\tau_2 P_2(\sin\phi)\left(\frac{3}{4}\sin^2\varepsilon - \frac{1}{2}\right) \\ & + \frac{5}{8}\tau_1 e P_2(\sin\phi)\left(\frac{3}{4}\sin^2\varepsilon - \frac{1}{2}\right)\cos(M_S - \psi) \\ & + \frac{3}{4}\tau_1 e P_2(\sin\phi)\sin^2\varepsilon \cos(2\omega_S + M_S - \psi) \ . \qquad (11)\end{aligned}$$

The observed values are $\tau_1 = 78.0$ °C., $\tau_2 = 234.8$ °C., and $\psi = 31.5°$ [*North et al.*, 1981, Table 1]. The amplitude τ_1 and lag angle ψ were actually found by North *et al.* only for the $P_1(\sin\varphi)$ [$\sin\varepsilon \sin(\omega_S + M_S - \psi)$] term; but they are assumed here to apply to all of the terms proportional to $e \cos(M_S - \psi)$ and $e \cos(2\omega_S + M_S - \psi)$ as well, since they have very nearly the same frequency, though this could be questioned because these terms apply

to different spherical harmonics. Also, *North et al.* [1981] calculated the value of τ_1 by symmetrizing the Earth. This assumes that temperatures observed in the northern hemisphere also apply to the southern hemisphere. Because the continents occur mostly in the northern hemisphere and show greater temperature variations than the oceans, their table presumably overestimates the temperature extremes on the real Earth. Further, *North et al.* [1981, p. 105] assume $t = 0$ at the northern hemisphere's winter solstice, while the present paper uses the angle $\omega_s + M_S$, which is zero at the vernal equinox, where the Sun is on the equator; thus the zero points differ by 90°. Hence in making comparisons with North *et al.*'s table, one must be careful to switch to the conventions used here.

Equations (10) and (11) will be used to investigate the properties of the NEBM in the next three sections. The diffusion constant D and an associated mystery are considered first.

4. Diffusion constant D

The diffusion constant D can be found by equating the time-invariant parts of the $P_2(\sin \phi)$ coefficients in (10), so that

$$D = \frac{4(1-A)Q - H_1\tau_2}{6\tau_2} = 0.119 \qquad (12)$$

The value derived (12) is much lower than the 0.649 found by *North et al.* [1981, p. 96] for their linear energy balance model; thus the present nonlinear model indicates that the overall heat transport is countered by other factors when averaging around the whole globe. This largely agrees with the result found in *Rubincam* [2004], where the equator-to-pole temperature difference on the real Earth is actually larger than that for the inertia-free gray body (1) with $A = 0.3$ and $\varepsilon_{IR} \approx 1$.

Clearly diffusion has importance for the real Earth: thanks to the Gulf Stream, London has a temperate climate, even though it is farther north than Winnipeg. So why is the diffusion constant (12) so small?

The resolution to the mystery presumably lies in continentality and albedo. While the Gulf Stream may heat Europe, continental interiors get cold; also, the albedo increases with latitude [e.g., *Stephens et al.*, 1981]. These last two would tend to counter the effects of winds and currents, which transport heat to the polar latitudes and moderate the equator-to-pole temperature difference. Thus the net effect is to give a small D in the simple model examined here.

The larger *North et al.* [1981] value for D indicates that latitudinal heat flow is substantial. The discrepancy between the NEBM and the linear energy balance model may come from the linear model's fitting an inherently curved set of data to the form $B_0 + B_1 T$, resulting in a large diffusion coefficient D, thus giving diffusion a spurious importance.

Short et al. [1991] investigate a linear energy balance model which includes continentality. A similar study using a nonlinear model to investigate the discrepancy in the D values would be interesting and worth pursuing, but this will not be done here.

5. Inconsistent values of C

Finding C from (10) and (11) is more complicated than finding D. Writing the $P_1(\sin \phi)$ part of ΔT in (11) the usual complex notation

$$\tilde{\tau}_1 \left[\frac{1}{2} P_1(\sin \phi) \sin \varepsilon \, e^{2\pi i t} \right]$$

and substituting in (10) yields

$$2\pi i C \tilde{\tau}_1 \; + \; 2D\tilde{\tau}_1 \; + \; H_1 \tilde{\tau}_1 \; = \; 4(1-A)Q$$

where $\dot{\omega}_S + \dot{M}_S \approx 2\pi$ (with time t measured in years), so that

$$\tilde{\tau}_1 = \tau_1 e^{-i\psi}$$

where

$$\tau_1 = \frac{4(1-A)Q}{\sqrt{(2D+H_1)^2 + (2\pi C)^2}} \tag{13}$$

and

$$\tan\psi = \frac{2\pi C}{2D+H_1} \tag{14}$$

Thus from (13) and (14) it can be seen that there are actually two equations involving C. Solving each equation for C using the observed values of H_1, τ_1, and ψ and the value for D found above yields inconsistent results: in one case $C = 1.76$ and $C = 0.33$ in the other. Fortunately the value for C is not needed in what follows below, and the observed values of τ_1 and ψ will simply be adopted in what comes next, rather than digress and follow up on the discrepancy; but it would be worth pursuing in the future.

6. Seversmith psychroterms

Proceeding to the second-order solution, the temperature can be written

$$T = T_0 + \Delta T + \delta T \tag{15}$$

where δT is the second-order part of the temperature, and the first-order part ΔT has already been given in (11). Substituting (15) into (10) and eliding the first-order solution leaves

$$C\frac{\partial(\delta T)}{\partial t} - \frac{\partial\left[D(1-\mu^2)\frac{\partial(\delta T)}{\partial \mu}\right]}{\partial \mu} + H_1\,\delta T + H_2(\Delta T)^2 \cong (1-A)\,\Delta F_S \qquad (16)$$

as the second-order equation. Now the $H_2(\Delta T)^2$ term produces cross-products, where ΔT is given by (11). With the aid of

$$P_0(\cos\phi)\,P_1(\cos\phi) = P_1(\cos\phi)$$

$$P_1(\cos\phi)\,P_2(\cos\phi) = [2P_1(\cos\phi) + 3P_3(\cos\phi)]/5$$

$$P_1(\cos\phi)\,P_4(\cos\phi) = [4P_3(\cos\phi) + 5P_5(\cos\phi)]/9$$

$H_2(\Delta T)^2$ can be written

$$3H_2\tau_1^2\,(e\sin\varepsilon\sin\omega_S)\,[P_1(\sin\phi) - \frac{1}{2}P_3(\sin\phi)]/16 \qquad (17)$$

plus other terms. The important thing to note about (17) is the appearance of $e \sin \omega_S$. Since terms of the sort (17) do not appear on the right side of (16), they must be cancelled by similar terms in δT in the other parts of (16).

The expression (17) above contains the long periods of $e \sin \omega_S$, so that $C\partial(\delta T)/\partial T$ changes slowly in (16) and can be neglected. To see this, assume δT can be written in the form $e^{2\pi i \nu t}$, where $\nu = 2\pi/23{,}000$ is the frequency associated with the 23 kyr period. Differentiating δT with respect to time brings the ν out in front of the term. Since ν is small compared to seasonal frequencies, the time derivative is small and can be ignored.

Hence the precession index part of the temperature can be solved for from

$$\frac{\partial\left[D(1-\mu^2)\dfrac{\partial(\delta T_{SP})}{\partial\mu}\right]}{\partial\mu} + H_1\,\delta T_{SP}$$

$$\simeq -3H_2\tau_1^2\,(e\sin\varepsilon\sin\omega_S)\,[P_1(\sin\phi) - \frac{1}{2}P_3(\sin\phi)]/16$$

producing

$$\delta T_{SP} \cong -e\,\sin\varepsilon\sin\omega_S\left(\frac{3H_2\tau_1^2}{32D+16H_1}\right)\left\{P_1(\sin\phi) - \frac{(2D+H_1)}{2(12D+H_1)}P_3(\sin\phi)\right\}. \qquad (18)$$

Substituting numerical values in (18) yields

$$\delta T_{SP} \cong -13.7\,e\sin\omega_S\,P_1(\sin\phi) + 5.1\,e\sin\omega_S\,P_3(\sin\phi)\ \ ^\circ\mathrm{C}. \qquad (19)$$

For e equal to the maximum value 0.06, δT_{SP} achieves extreme values of $\delta T_{SP} = \pm 0.64^\circ$ C. when $\omega_S = 90^\circ, 270^\circ$ and $\varphi = \pm 48.5$. At $\varphi = +48.5^\circ$, this becomes $-10.67\,e\sin\omega_S$ °C.

The results for the NEBM are graphed in Figure 3. Figure 4 illustrates the fact that the perihelion hemisphere is the cooler.

It must be noted that (18) depends on the value for τ_1, which is probably overestimated; see the remarks after (11). Hence the magnitude of the first term in (19) is may be too big. Also, including more terms in (11) will produce more terms in (18). Equation (18) is limited because (11) is limited to the few terms in the spherical harmonic expansion of temperature for which numerical values may be reasonably assumed.

7. Comparison to obliquity changes

The result (19) can be compared to the ΔT_{obl} expected from obliquity changes. From (11) the second harmonic in temperature is

$$\frac{5}{16}\tau_2 P_2(\sin\phi)\left(\frac{3}{4}\sin^2\varepsilon - \frac{1}{2}\right)$$

This will give changes in temperature as the obliquity changes with the 41 kyr period of magnitude by Taylor series $\Delta T \approx (\partial T/\partial\varepsilon)\Delta\varepsilon$

$$\Delta T_{obl} = \frac{5}{16}\tau_2 P_2(\sin\phi)\left(\frac{3}{2}\sin\varepsilon\cos\varepsilon\right)\Delta\varepsilon \qquad (20)$$

where $\Delta\varepsilon$ is the change in obliquity. Because $\Delta\varepsilon \approx \pm 1°$over the obliquity cycle [e.g., *Hays et al.* 1976; *Berger et al.* 1984; *Hinnov* 2000],

$$\Delta T_{obl} \approx 40.2\,\Delta\varepsilon \approx \pm 0.7\ \text{K}, \qquad (21)$$

At maximum e the Seversmith psychroterms give ± 0.64° C by (19) and are thus 90% the size of the obliquity variation. These calculations of course assume no feedback mechanisms, such as ice-albedo feedback.

8. Temperature schematic

Figure 5 illustrates the temperature change with and without the Seversmith psychroterms. In this figure $\phi = +48.5°$ (about the same latitude as the U.S.-Canadian border), while e fixed at 0.06. As mentioned above, these values of ϕ and e are chosen to maximize the δT_{SP} in (19).

Part (a) of Figure 5 shows the temperature variation as a function of time without the psychroterms. Here the temperature variation ΔT is represented by terms which have just two of the many frequencies which appear in the insolation:

$$\Delta T \approx 30\, e \cos M_S + 11.6 \sin (\omega_S + M_S) \quad °C. \tag{22}$$

This equation is based on (7), and omits the lag angle ψ. The amplitude of the sin $(\omega_S + M_S)$ term, which is an annual term (equinox to equinox), comes from observing that for the whole Earth this term is 15.5 $P_1(\sin \phi)$ sin $(\omega_S + M_S)$ °C, again ignoring the lag angle [*North et al.*, 1981, p. 100]; setting $\phi = +48.5°$ gives the amplitude in the equation above. The e cos M_S term, which cycles through 360° from perihelion to perihelion, is not observed separately because its period is nearly one year, making it difficult to distinguish from the annual term; instead by (11), its amplitude is scaled from the annual term, on the presumption that terms which have very nearly the same frequency should scale linearly with their importance in the insolation; however, see the caveats associated with (11) above.

In Figure 5(a) the frequency difference between the sin $(\omega_S + M_S)$ and e cos M_S is grossly exaggerated to make visible on the plot. The actual rate of change in ω_S is small; in

reality $\dot{\omega}_S \approx +62$ arc s yr^{-1} [e.g., *White et al.*, 1996]. Hence Figure 5 is schematic; the plotted amplitudes are realistic, but the frequencies are not, and only a few of the thousands of cycles are shown. The peaks show summer temperatures at this latitude, with summers being hottest when the Sun's perigee ω_S is near 90° and coldest near 270°, thanks to the presence of the $e \cos M_S$ term. Similarly, the valleys show winter temperatures; winters are coldest at this latitude for $\omega_S \approx 90°$ and warmest for $\omega_S \approx 270°$.

Note that there is a beat between the two terms, and that this beat period has the same period as $e \sin \omega_S$, about 23 kyr. However, this frequency does not actually appear in the temperature equation above; in a signal there is a difference between the frequency of the envelope and the carrier wave. In the Milankovitch model, the peaks in Figure 5(a) are deemed to be important, and if only the peaks were plotted, a sinusoid with the 23 kyr period would result. However, this "strobing" at selected points in Figure 5(a) is to manipulate a curve which contains only short-period sin $(\omega_S + M_S)$ and $e \cos M_S$ terms into giving the precession index frequency [*Rubincam*, 2004]. And to focus only on the peaks as important for northern ice sheet growth is to assume a nonlinear climate model; a linear climate model would contain only the original short-period annual and near-annual frequencies.

Part (b) of Figure 5 shows the same terms as part (a), but with the addition of the Seversmith psychroterms discussed here. As has been shown in Section 3, for the NEBM this term is $-10.67\, e \sin \omega_S$ °C. at the chosen latitude; the new term is displayed as the long-period sine curve which hugs zero. Note that its amplitude is about 1/3 that of the $e \cos M_S$ term. Unlike the curve shown in (a), the new term has a true $e \sin \omega_S$ period, so that there is a long-period heating and cooling. The new equation for ΔT graphed in (b) is thus

$$\Delta T \approx 30\, e \cos M_S + 11.6 \sin (\omega_S + M_S) - 10.67\, e \sin \omega_S \quad °C. \qquad (23)$$

This graph is to be compared with (a). The differences are small, and are best seen by comparing how far the peaks rise above the $\Delta T = +10°$ C. line and how far the valleys fall below the $-10°$ C. line. For the peaks, it will be noted that the new effect works in opposition to the $e \cos M_S$ term, making the hot northern summers a little cooler and the cool summers a little hotter. Hence if the Milankovitch mechanism works, it must overcome the moderating influence of the new effect.

On the other hand, examination of the valleys indicates that the Seversmith psychroterms make the cold northern winters even colder and the warm winters even warmer. Figure 4 summarizes the situation with respect to both the northern and southern hemispheres, and summer and winter. One could argue that these results support James Croll's idea that it is very cold northern winters which cause enough ice to accumulate to last through the summer [e.g., *Pisias and Imbrie*, 1986], rather than the cool summers in the Milankovitch model.

But rather than support Croll, instead it is hypothesized below in the Discussion section that it is the long-term hemispheric heating and cooling which might cause the ice sheets to grow. While *Imbrie et al.* [1988] argue for northern hemisphere control of the northern ice sheets, the effect presented here perhaps argues for southern hemisphere control of the northern ice sheets. The idea is that during the times when ω_S is near 270°, the southern hemisphere undergoes a long-term cooling, especially the southern oceans and perhaps the Antarctic ice cap. The cold water slowly makes its way north, cooling the whole Earth and eventually producing the northern ice sheets.

9. Ice ages and the precession index

The precession index in temperature reveals itself as the product of short-period terms in these $(\Delta T)^2$ models. This is shown in Figure 6 in a highly schematic diagram of the insolation spectrum and the temperature spectrum. The Earth's nonlinear climate

system creates the precession index line from the insolation. It is chiefly the $P_0(\sin \varphi)$ [e cos M_S] term in F_S multiplying the strong annual term $P_1(\sin \varphi)$[sin ε sin $(\omega_S + M_S)$] which produces $P_1(\sin \varphi)$ [e sin ω_S], giving the long periods of 23 kyr and 19 kyr. It is extremely interesting to note that as far as long periods are concerned, the only cross-product terms of any significance are these e sin ω_S terms: there are no e sin $2\omega_S$ or e to the first power terms, for instance.

The magnitude of the effect is fairly large: for the energy balance model it is ±0.64 °C. at maximum eccentricity and without ice-albedo feedback. For comparison, the difference in the global temperature between the present and the last glacial maximum was about –4° C. [*Crowley*, 1983, p. 868]. The obliquity oscillation gives ±0.7 °C. without feedback (see (21) above), so that the Seversmith psychroterms can get nearly as large as the one induced by obliquity variations.

The sign of the new mechanism appears paradoxical: when $\omega_S = 90°$ in (19), the Sun is close to the Earth at northern summer solstice, producing a long-term cooling in the northern hemisphere with simultaneous warming in the southern [*Rubincam*, 2004]. Similarly, when $\omega_S = 270°$, the Sun is far from the northern hemisphere during northern summer and this effect produces a long-term warming in the north, while at the same time the southern hemisphere undergoes long-term cooling. This is counter to intuition, which says that when the Sun is close to the northern hemisphere during northern summer that hemisphere ought to warm, not cool. However, it is the short period e cos M_S term in (11) which does the warming in accordance with intuition. The peculiar sign of the mechanism presented here is in fact correct and necessary to achieve energy balance in the nonlinear models. In fact any model which radiates in the infrared like T^n, where $n > 1$, will give a paradoxical e sin ω_S term.

The sign is counter to that of the standard Milankovitch explanation of why the precession index is important. The standard model relies on the short period terms: it calls for cool northern summers when ω_S is near 270° and the Sun is far from the Earth, so that

snow lingers through the summers, ultimately building up into an ice sheet [e.g., *Milankovitch*, 1941, pp. 435-436; *Pisias and Imbrie*, 1986, p. 45]. By warming the northern cool summers somewhat and heating a little the cool winters (see Figure 4), the effect found here presumably makes it harder for the standard model to operate. If the standard explanation is responsible for the waxing and waning of ice sheets at the 23 kyr and 19 kyr periods, then it must be more efficient than previously thought to overcome the present mechanism with its opposing sign [*Rubincam*, 2004].

In contrast to smoothing out the summer temperatures, the new effect exaggerates the northern winter temperatures, making the cool winters colder and the warm winters warmer. Scottish geologist James Croll suggested in the 1860s that colder northern winters were the key to ice sheet growth [e.g., *Pisias and Imbrie*, 1986, p. 45]. Croll's suggestion was later dropped in favor of *Milankovitch's* [1941] cool summers. Hence one could use the new effect to argue that perhaps Croll was correct, rather than Milankovitch. However, Croll's case will not be argued here.

It may be that neither the Croll nor the Milankovitch mechanisms are responsible for the precession index ice growth and decay; rather, it is hypothesized that the long-term heating and cooling of the southern hemisphere controls the northern ice sheets [*Rubincam*, 2004]. This is illustrated in Figure 7.

Figure 7 is the same as Figure 5, except that it shows temperature in the southern hemisphere at $\phi = -48.5°$. In this case the southern hemisphere undergoes a long-term cooling when the Sun is near $\omega_s = 270°$, as shown in Figure 7(b) by the small but long wavelength sinusoid. The idea is that the southern oceans cool when the Sun is far from the Earth during northern summer. Thus, the southern oceans stay cool for a long time, perhaps allowing sea ice to be accumulated. The high albedo of the ice cools the southern hemisphere even more, so that ice-albedo feedback takes place [e.g., *Gildor and Tziperman*, 2000, 2001], and the southern waters get very cold. The cold water slowly flows north,

eventually cooling the northern hemisphere enough to build up ice there. This hypothesis of course goes far beyond the simple NEBM discussed in the present paper.

Is there observational support for the southern ocean hypothesis in the paleoclimate data? *Imbrie et al.* [1988, p. 145] show the phase lag for cold-season sea surface temperatures with respect to the orbital forcing for 16 sites in the North and South Atlantic and one in the Indian Ocean. Figure 8 (which is based on Imbrie *et al.'s* figure) summarizes their findings. In this diagram zero phase lag points to the top of the page, which corresponds to $\omega_S = 90°$, so that the Sun is close to the northern hemisphere during northern summer, making the northern summers hot. The arrow labeled "MI" points to the phase of minimum ice volume associated with the precession index. Phase is measured clockwise from the top of the page, so that the minimum ice volume lags the orbital forcing by about 90°, according to Imbrie et al.'s convention; a 90° phase lag is what would be expected on a water-rich planet [e.g., *Rubincam*, 1995, p. 371]. Because the precession index has a predominantly 23 kyr period, the 90° phase lag means a time delay of about 6 kyr. The shaded area shows the range of southern hemisphere phase lags as recovered from the 17 ocean-bottom core samples, while the striped area shows the range of northern hemisphere phase lags. There is a wide range of phase lags in the data, but they show a clear difference between the response times of the two hemispheres: the northern hemisphere significantly lags the south when it comes to the forcing. In terms of time, the delay is roughly 5 kyr.

These data appear to support the hypothesis. When the Sun is close to the Earth during northern summer ($\omega_S \approx 90°$), there is a long-term warming in the southern hemisphere; thus the southern oceans should warm first, as observed. The warm waters flow north, warming the northern hemisphere. Since the turn-over time of the oceans is a few thousand years, a time delay of a few kyr would be expected between hemispheres. The data give approximately 5 kyr, in apparent agreement with the hypothesis.

The above argument deals with warming. One would expect a similar scenario to hold for cooling and the growth of ice sheets, with the southern hemisphere undergoing a long-term cooling when the Sun is far from the Earth during northern summer ($\omega_S \approx 270°$), with the cold water spreading north in a few thousand years, cooling the northern hemisphere and allowing ice to build up in North America and Eurasia.

There is also some support for this hypothesis in the analogous phase wheel for the 41 kyr-period obliquity forcing, which is shown in Figure 9; this figure is based on *Imbrie et al.'s* [1988, p. 146]. Here the phase is zero at maximum obliquity, when the poles see the most Sun. As in Figure 8, the diagram tends to show the southern hemisphere warming first, followed by the northern. The separation of phase lags is not as clear-cut as for the precession cycle, but this might be expected. Unlike the precession effect found here, the insolation and temperature variation during the obliquity cycle treats both hemispheres equally, as seen from (3) and (20); $P_2(\sin \phi)$ is symmetrical about the equator. So the fact that there is a difference at all in the response times of the hemispheres during the obliquity cycle, with the southern hemisphere leading, again argues for southern hemisphere control. Thus there seems to be something special about the southern hemisphere, presumably having to do with sea ice around Antarctica; so a sea ice model [*Gildor and Tziperman*, 2000; 2001] may be of some interest.

Imbrie et al. [1988] favor northern hemisphere control of ice sheets *à la* Milankovitch. They realize that this causes a problem with regard to the precession index, but reject southern hemisphere forcing as "undesirably complex" [p. 154]. However, as shown in Figures 8 and 9, which are based on Imbrie *et al.*'s own diagrams, both the precession index and the obliquity cycle may be controlled by the southern hemisphere.

It should also be noted that the above development was with regard to temperature only; no ice was included. Hence the psychroterms will exist even on an ice-free world [*Rubincam*, 2004].

10. Discussion

Global climate models (GCMs) seek to include the greatest possible details in simulating climate. This comes at the expense of achieving easy physical insight, due to including the wealth of effects, and being forced to run numerical simulations [e.g., *North et al.*, 1981, p. 91]. In contrast, the purpose of energy balance models is to examine climate from the simplest possible perspective in order to gain understanding of the basics of the climate system. It would certainly be difficult to discover the Seversmith psychroterms without at least a crude analytical solution to some simple-minded model like the NEBM.

However, energy balance models have numerous shortcomings. The heat storage term $C\partial T/\partial t$ in (4) is presumably meant to be analogous to the similar term in the heat conduction equation $\rho C\partial T/\partial t = K\nabla^2 T$; but it is not clear what the term means physically; (4) certainly does not specifically allow for heat conduction into the ground. Also, the relationship between surface temperature (5) and outgoing infrared radiation is empirically observed and not well motivated conceptually. Moreover, the diffusion constant D must be solved for as in (12), and by (13) and (14) the data give inconsistent values for C.

Given these difficulties, the best approach may be to use rudimentary physical models with parameters whose values are already known; an example would be vertical heat conduction into the ground on an atmosphere-free planet with an assumed conductivity, density, etc. The results could then be compared to observation. Any disagreement between the two might indicate how to improve the model, such as to include at the next attempt some simple representation of an atmosphere.

The problem with this approach is that the program may be difficult to carry out. Even the most elementary parameters may not be known a priori, and model complexity may increase rapidly. But it might be better than solving for the parameters of a poorly motivated model from the data: if the model is not very meaningful, what meaning can be

attached to the solved-for parameters? For instance, solving for D in the linear energy balance model gave a value that was much too large (section 4 above).

Even assuming (4) with all its shortcomings, obstacles arose in trying to find a solution to the NEBM. The gray body without thermal inertia has relatively easy solution. It has an analytical form similar to that of the insolation (2):

$$T(\phi,\lambda,\eta)=\left(\frac{(1-A)F_S^0 r_0^2}{\varepsilon_{IR}\sigma a^2}\right)^{1/4}\sum_{\ell=0}^{+\infty}c_\ell\sum_{m=0}^{\ell}(2-\delta_{0m})\frac{(\ell-m)!}{(\ell+m)!}$$

$$\bullet\sum_{p=0}^{\ell}\sum_{q=-\infty}^{+\infty}F_{\ell mp}(\varepsilon)W^{bb}_{\ell-2p,q}(e)P_{\ell m}(\sin\phi)$$

$$\bullet\begin{bmatrix}\cos\\ \sin\end{bmatrix}_{\ell-m\ \text{odd}}^{\ell-m\ \text{even}}[(\ell-2p)\omega_S+(\ell-2p+q)M_S+m(\Omega_S-\eta-\lambda)] \qquad (24)$$

[*Rubincam*, 2004], where the superscript "bb" on $W^{bb}_{\ell-2p,q}(e)$ stands for "black body" and is used to distinguish these eccentricity functions from those associated with the insolation, which are written without the superscript. Also, the values for c_ℓ in the above equation are not the same as those for d_ℓ in (2).

In contrast to the gray body, no complete analytical solution to the NEBM equation (4) is known. Instead, an approximation based on an iterative solution to order $(\Delta T)^2$ was employed, and finding more than a few terms this way can be cumbersome. As a result, while the Seversmith psychroterms could be found to a certain level of approximation, it is not presently known how the $P_0(\sin\phi)$ temperature term in the NEBM, when averaged over latitude, longitude, and time, behaves with e^2.

In the gray body (24) average temperature paradoxically goes down as e^2 increases, while the average insolation goes up. Specifically, if the angular brackets $\langle T\rangle$ mean averaging over the Earth's surface and the bar ($\overline{T}$) means averaging over time, then

$$\langle \overline{T} \rangle \propto 1 - \frac{e^2}{16} \tag{25}$$

to order e^2 for the gray body, while

$$\langle \overline{F_S} \rangle \propto 1 + \frac{e^2}{2} \tag{26}$$

to the same order. The paradox is resolved by noting that

$$\langle \overline{F_S} \rangle \propto \langle \overline{T^4} \rangle \neq \langle \overline{T} \rangle^4, \tag{27}$$

so that while the average temperature goes down as e^2 increases as shown in (25), periodic terms are squared, cubed, and taken to the fourth power in the middle expression in (27), so that the power balance (26) is maintained.

Is the same "paradoxical" behavior true of the NEBM? The answer is not known at present, because it is not yet clear how many iterative solutions of (4) must be found and how many terms must be retained before a reliable result similar to (25) can be achieved.

Adding to the difficulties are the unknowns in (11); that equation was used to help find the psychroterms. Some of the terms in (11) had to be guessed at, due to a lack of data.

The slow ocean currents discussed in section 9 are of course not present in the model discussed here, nor are continents and ice-albedo feedback [*North et al.*, 1981, 1983; *Graves et al.*, 1993; *Short et al.*, 1991]. The continents and feedback presumably amplify the effect. Ice-albedo feedback may amplify the Seversmith psychroterms to 1 or a few °C., which might be enough for ice sheet growth. Moreover, it may be the psychroterms which

triggers the ice ages which come and go with eccentricity e [*Rubincam*, 2004]; in other words, $e \sin \omega_S \rightarrow e$ via some nonlinear process. These all represent avenues for future research.

Because the Earth surely radiates infrared energy back into space like T^n, where $n > 1$, the mechanism discussed above must certainly exist. However, the δT_{SP} found here may not be "the" precession index; some other nonlinear mechanism rather than the one discussed above may be stronger and be the main reason for the importance of $e \sin \omega_S$ for the ice ages. The traditional Milankovitch "model" is one possibility. The change in Hadley cell circulation as proposed by *Lindzen* [1994] and *Lindzen and Pan* [1994] is another. There are undoubtedly others.

Acknowledgments

I have enjoyed profitable discussions with Bruce G. Bills. I thank Katy Gammage, Jay O'Leary, and Brad Lee for producing the figures.

References

Berger A, Imbrie J, Hays J, Kukla G, Saltzman B (editors) (1984) Milankovitch and Climate. Dordrecht, Netherlands: D. Reidel, 510 pp

Berger, A (1996) Comments to "Insolation in terms of Earth's orbital parameters" by D. P. Rubincam. Theor. Appl. Climatol. 53: 253-255

Caputo M (1967) The Gravity Field of the Earth. New York: Academic Press, 202 pp

Crowley, TJ (1983) The geologic record of climate change. Rev. Geophys. Space Phys. 4: 828-877

Gildor H Tziperman E (2000) Sea ice as the glacial cycles' climate switch: role of seasonal and orbital forcing. Paleoceanography 15: 605-615

Gildor H Tziperman E (2001) A sea ice climate switch mechanism for the 100-kyr glacial cycles. J. Geophys. Res. 106, 9117-9133

Graves C.E. Lee W-H North GR (1993) New parameterization and sensitivities for simple climate models. J. Geophys. Res. 98: 5025-5036

Hays JD Imbrie J Shackleton NJ (1976) Variations in the Earth's orbit: pacemaker of the ice ages. Science 194: 1121-1132

Hickey JR Alton BM Kyrle HL Hoyt D (1988) Total solar irradiance measurements by ERB/NIMBUS-7, a review of nine years. Space Sci. Rev. 48: 321-342

Hinnov L (2000) New perspectives on orbitally forced stratigraphy. Ann. Rev. Earth Planet. Sci. 28: 419-475

Humphreys WJ (1964) Physics of the Air. New York: Dover, 676 pp

Imbrie JA McIntyre A Mix A (1988), Oceanic response to orbital forcing in the late Quaternary: observational and experimental strategies, in *Climate and Geo-Sciences*, edited by A. Berger, S. Schneider, and J. Cl. Duplessy, pp. 121-164, Kluwer, Boston

Kaula WM (1966) Theory of Satellite Geodesy. Waltham, Mass.: Blaisdell, 124 pp

Lindzen RS (1994) Climate dynamics and global change. Ann. Rev. Fluid Mech. 26: 353-378

Lindzen RS Pan W (1994) A note on orbital control of equator-pole heat fluxes. Climate Dynamics 10: 49-57

Milankovitch M (1941) Canon of insolation and the ice-age problem. Royal Serbian Academy Special Publication 132. (English translation by the Israel Program for Scientific Translations, Jerusalem, 1969)

North GR Cahalan RF, Coakley JA (1981) Energy balance climate models. Rev. Geophys. Space Phys. 19: 91-121

North GR Mengel JG Short DA (1983) Simple energy balance model resolving the seasons and the continents: application to the astronomical theory of the ice ages. J. Geophys. Res. 88: 6576-6586

Pisias NG Imbrie J (1986) Orbital geometry, CO_2, and Pleistocene climate. Oceanus 29 [4]: 43-49

Rubincam DP (1994) Insolation in terms of Earth's orbital parameters. Theor. Appl. Climatol. 48: 195-202

Rubincam DP (1995) Has climate changed the Earth's tilt? Paleoceanography 10: 365-372

Rubincam DP (1996) Reply to comment on "Insolation in terms of Earth's orbital parameters." Theor. Appl. Climatol. 53: 257-258

Rubincam, D P (2004) Black body temperature, orbital elements, the Milankovitch precession index, and the Seversmith psychroterms. Theor. Appl. Climatol., *in press*

Short DA Mengel JG Crowley TJ Hyde WT North GR (1991) Filtering of Milankovitch cycles by Earth's geography. Quat. Res. 35: 157-173

Stephens GL Campbell GG Vonder Haar TJ (1981) Earth radiation budgets. J. Geophys. Res. 86: 9739-9760

White OR Mende W Beer J (1996) Testing for bias in the climate record. Science 271: 1880-1881

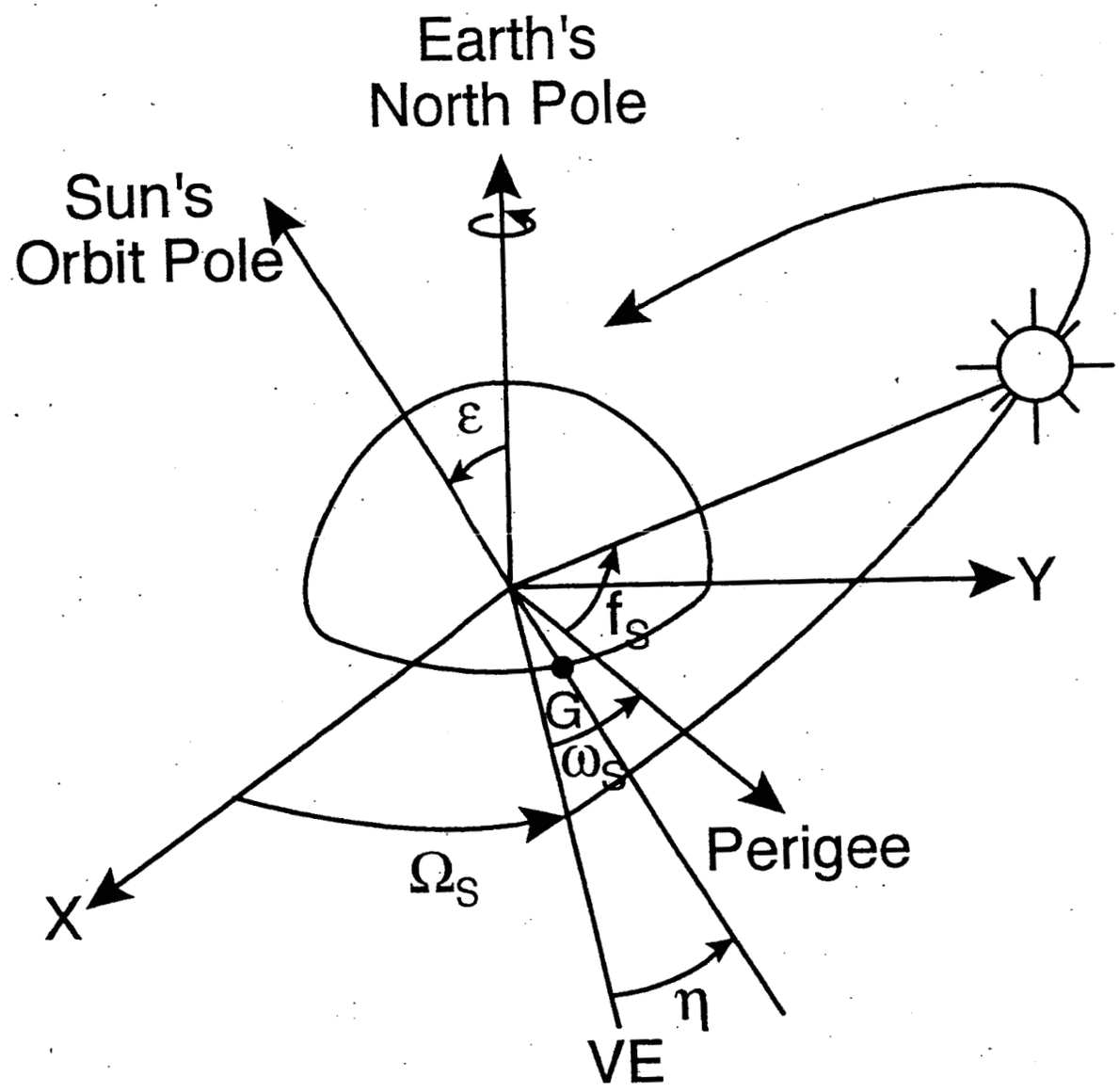

Figure 1

Geometry of the Sun's orbit about the Earth. Here ε = obliquity, ω_S = argument of perigee, Ω_S = node, and f_S = true anomaly. The point marked "G" on the equator marks the longitude of Greenwich; η is Greenwich sidereal time measured from the vernal equinox VE. The subscripts "S" distinguish the Earth-based frame used here from a solar-based frame. Note that $\omega_S = 90°$ when perihelion occurs at northern summer solstice and $\omega_S = 270°$ when aphelion occurs at northern summer solstice. Mean anomaly M_S is not shown.

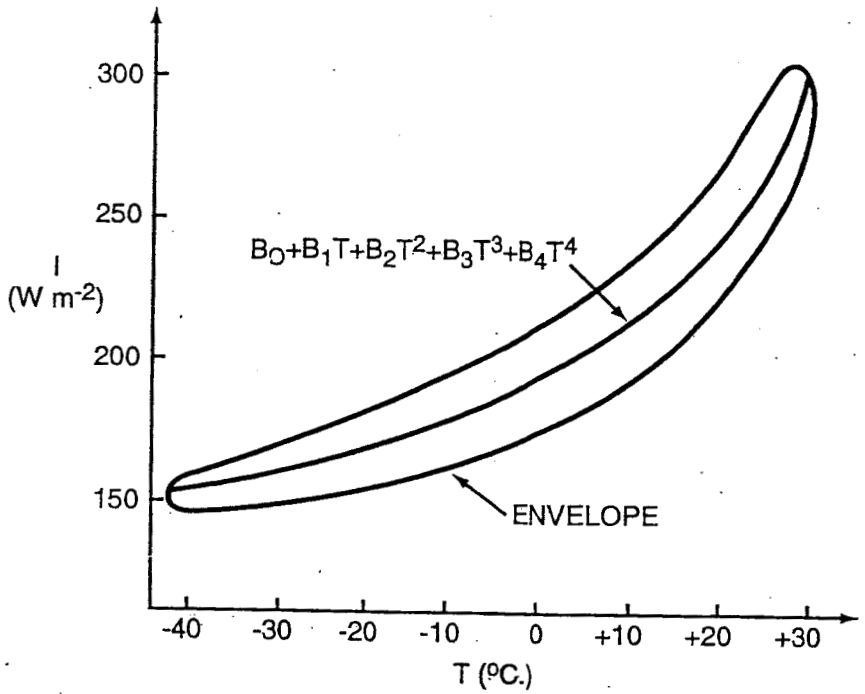

Figure 2

The outgoing infrared radiation as a function of temperature, based on Figure 1 of *Graves et al.* [1993]. The curve, which is a polynomial in T, is chosen to bisect the envelope. It is the curvature which gives rise to $e \sin \omega$ in temperature; a straight line would not do so.

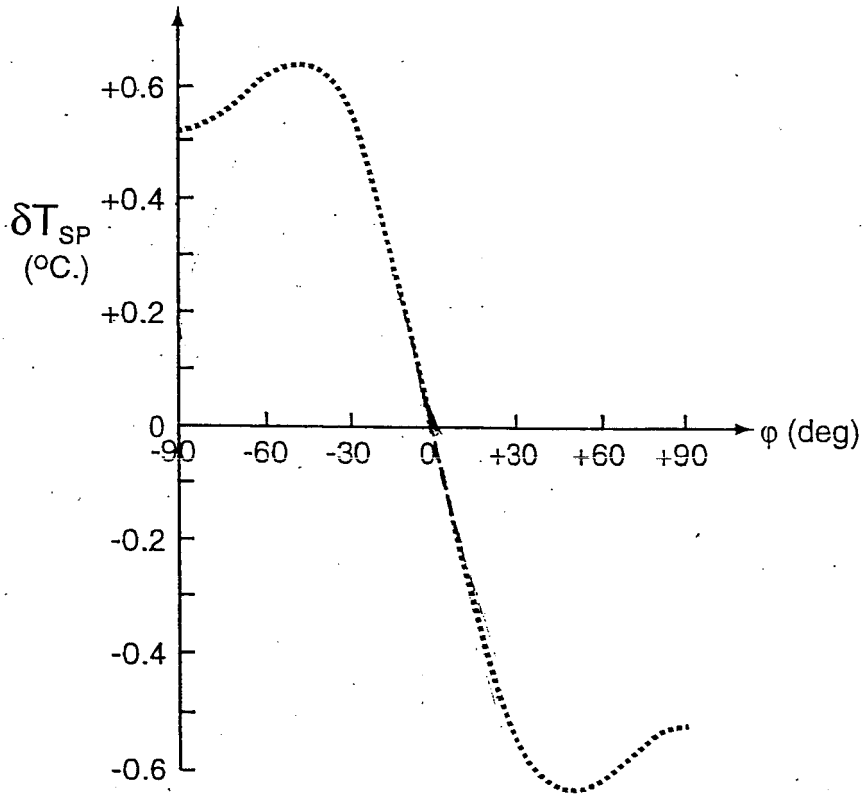

Figure 3

δT_{SP} for the energy balance model as a function of latitude φ for $e = 0.06$ and $\omega_S =$ 90° in (19). These values give the maximum changes in temperature.

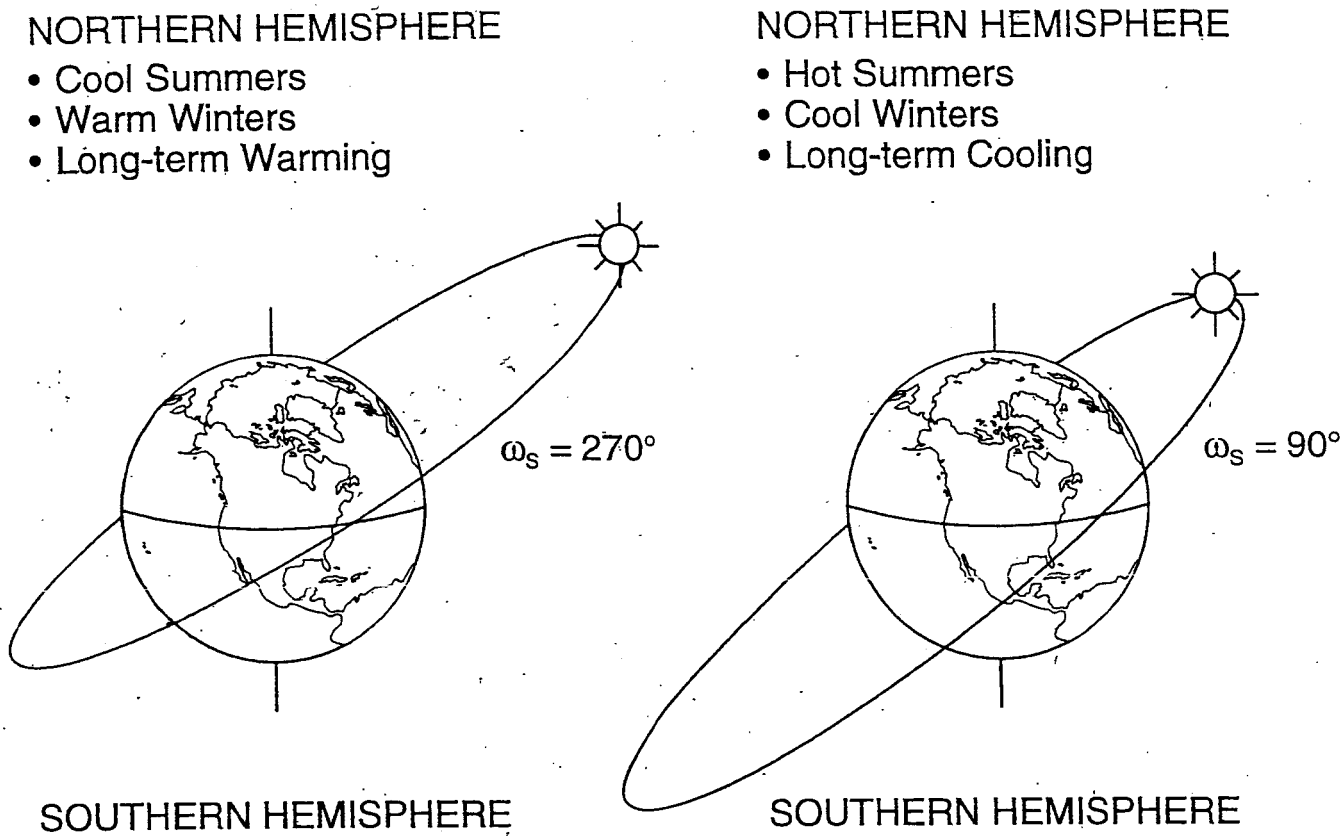

Figure 4

Summary of the long-term heating and cooling for the northern and southern hemispheres when $\omega_s = 90°$ and 270°, due to the psychroterm effect discussed here. "Long-term" means on the $e \sin \omega_s$ timescale. Note that the convention used here has $\omega_s = 90°$ when perihelion occurs at northern summer solstice and $\omega_s = 270°$ when aphelion occurs at northern summer solstice.

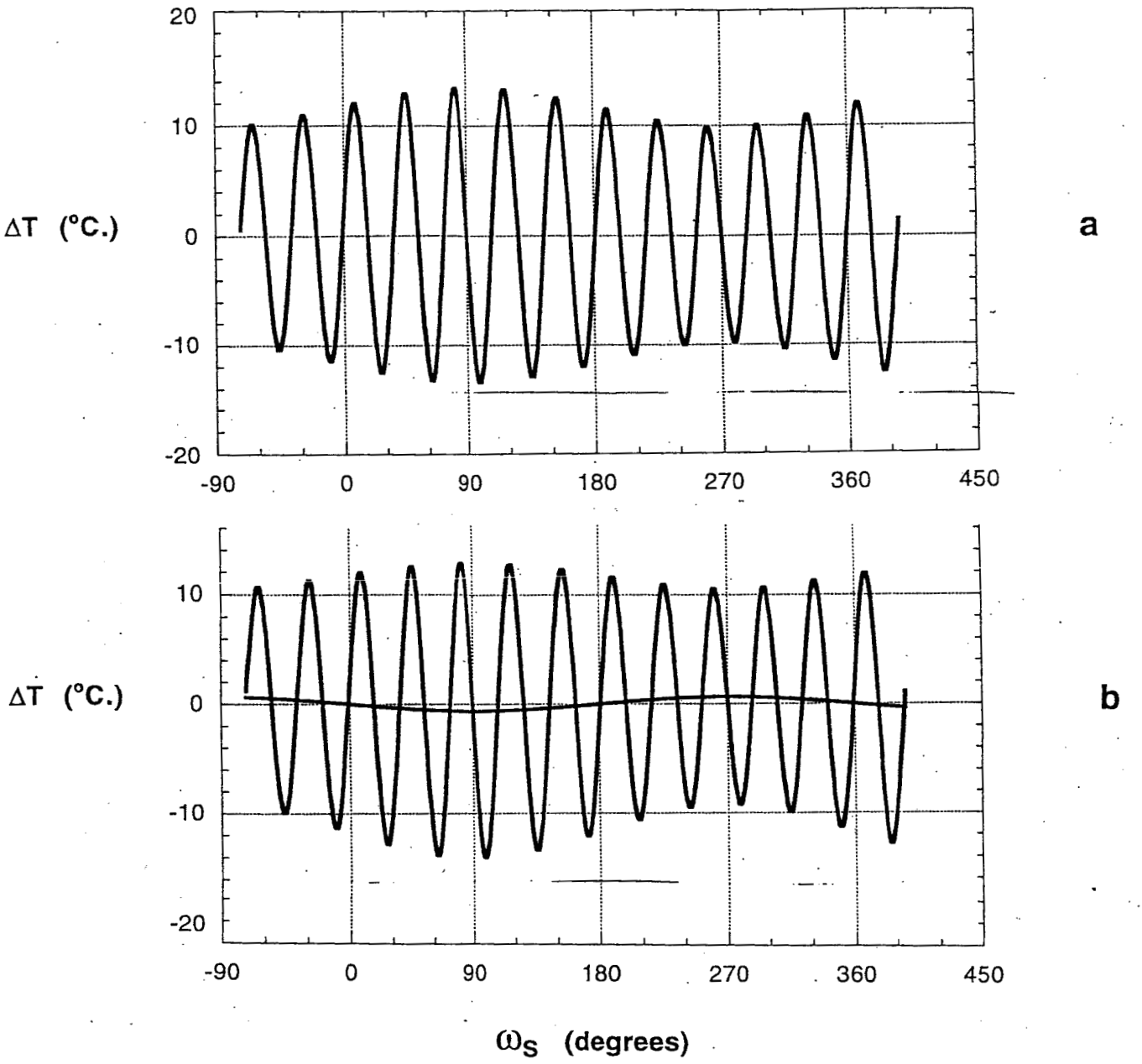

Figure 5

Schematic temperature variation ΔT at $\phi = +48.5°$. (a) For the $e \cos M_S$ and $P_1(\sin \phi)$ [sin $(\omega_S + M_S)$] terms only, with $e = 0.06$. (b) For the $e \cos M_S$, $P_1(\sin \phi)$ [sin $(\omega_S + M_S)$], and $e \sin \omega_S$ terms only, with $e = 0.06$. The $e \sin \omega_S$ term is also shown as the small-amplitude sine wave. Note that the $e \sin \omega_S$ term gives a long-term warming at this northern hemisphere location when $\omega_S \approx 270°$.

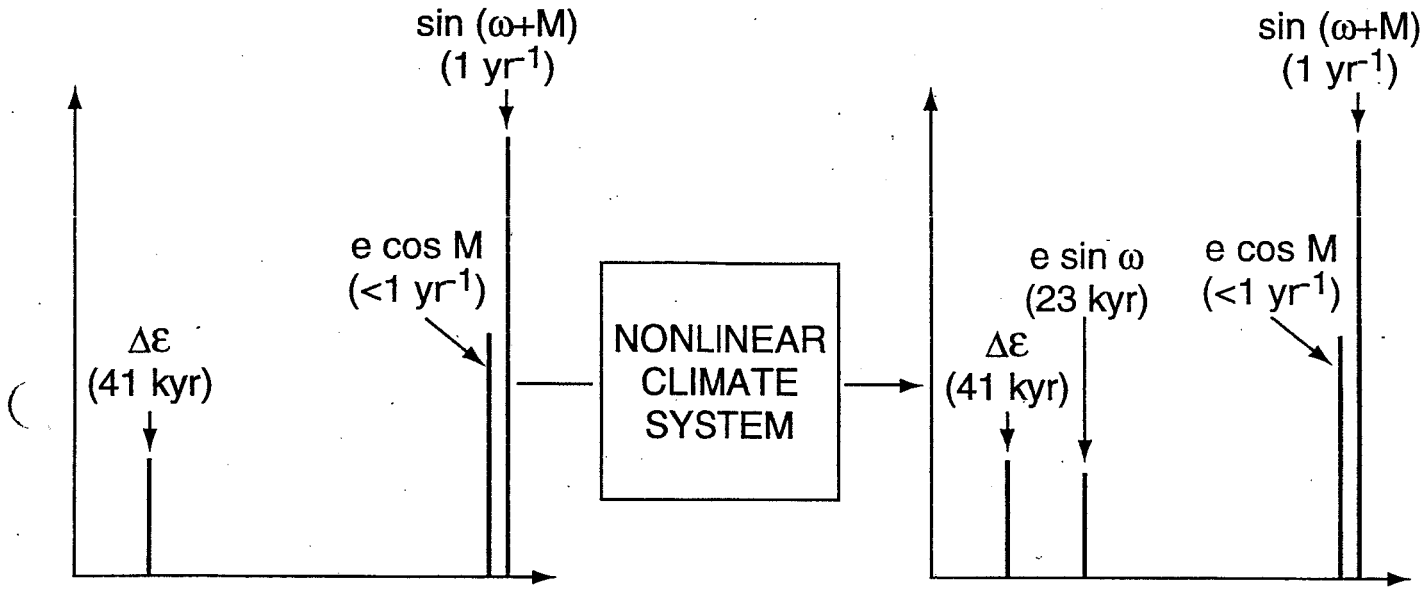

Figure 6

Schematic spectrum of insolation and temperature. This diagram shows how the Earth's nonlinear climate system manufactures a new spectral line in temperature from existing lines in insolation. The precession line is shown only as a single peak, and many other spectral lines are omitted for clarity.

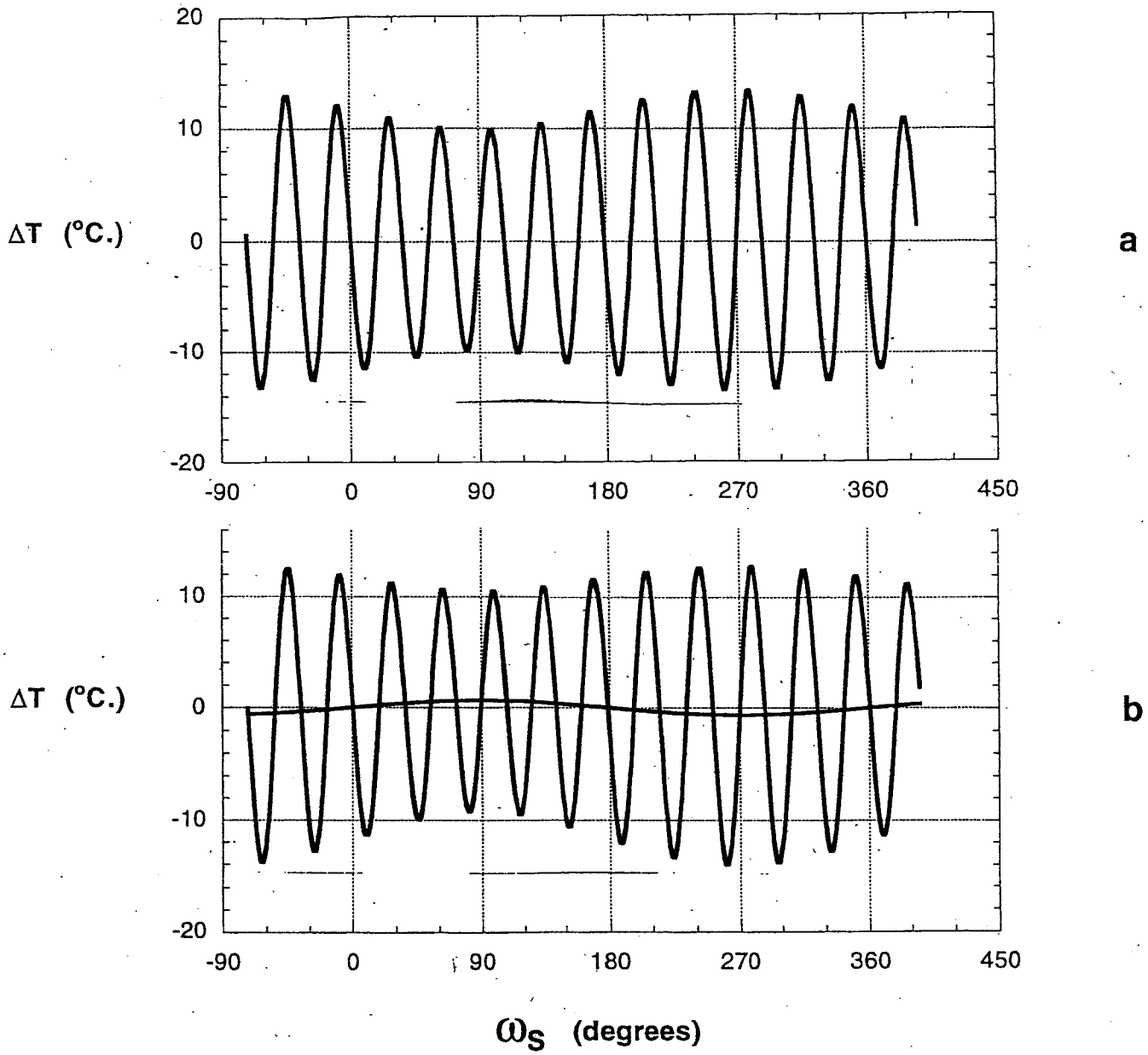

Figure 7

Schematic temperature variation ΔT at $\phi = -48.5°$. (a) For the $e \cos M_S$ and $P_1(\sin \phi)$ $\sin (\omega_S + M_S)$ terms only, with $e = 0.06$. (b) For the $e \cos M_S$, $P_1(\sin \phi)$ [$\sin (\omega_S + M_S)$], and $e \sin \omega_S$ terms only, with $e = 0.06$. The $e \sin \omega_S$ term is also shown as the small-amplitude sine wave. Note that the $e \sin \omega_S$ term gives a long-term cooling at this southern hemisphere location when $\omega_S \approx 270°$.

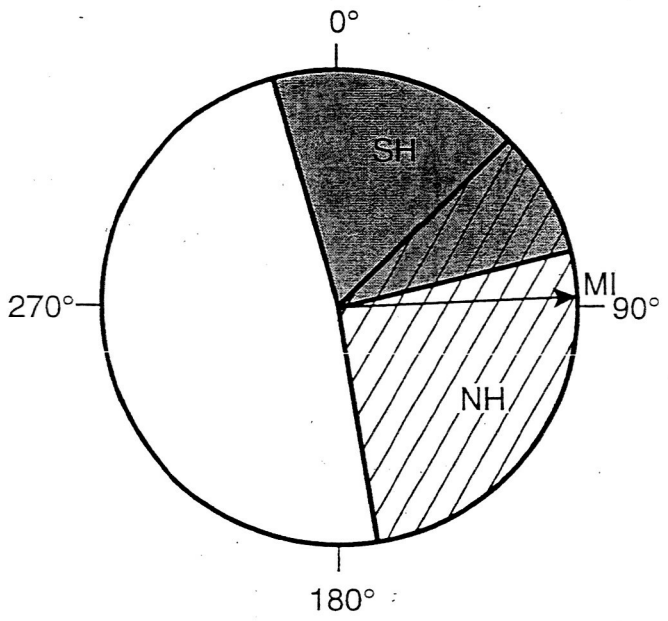

Figure 8

Phase wheel for the precession index for cold-season sea surface temperatures and for ice volume for 16 sites in the North and South Atlantic and one in the Indian Ocean. Hot northern summers ($\omega_s = 90°$) are at the top of the wheel at a phase lag of zero. The thick arrow marked "MI" is the phase lag for minimum ice volume. The phase lags for the southern hemisphere (SH) sites fall within the shaded area. The phase lags for the northern hemisphere (NH) sites fall within the striped area. The northern hemisphere clearly lags the southern when responding to the orbital forcing.

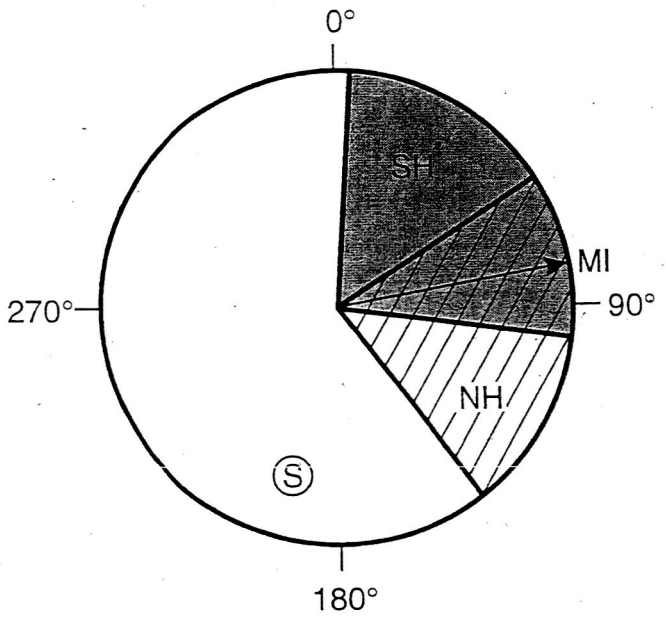

Figure 9

Phase wheel for the obliquity cycle for cold-season sea surface temperatures and for ice volume for the same 17 sites as in the previous figure. Maximum obliquity is at the top of the wheel at a phase lag of zero. The thick arrow marked "MI" is the phase lag for minimum ice volume. The phase lags for the southern hemisphere (SH) sites fall within the shaded area, except for a single southern hemisphere site (marked "S" within a circle) which occurs near a phase lag of 190°. The phase lags for the northern hemisphere (NH) sites fall within the striped area. The northern hemisphere tends to lag the southern when responding to the orbital forcing.